Investigation of T_1-Relaxation for OCS Rotational Transitions by Self- and Nonpolar Foreign Gas Collision

H. Mäder

Abteilung Chemische Physik im Institut für Physikalische Chemie der Universität Kiel

Z. Naturforsch. **34a**, 1170–1180 (1979); received August 16, 1979

The pressure dependence of $1/T_1$ has been measured at temperatures $\simeq$ 300 K and $\simeq$ 200 K for the carbonyl sulfide $J, |M| = (0, 0)$–$(1, 0)$, $(1, 0)$–$(2, 0)$, $(1, 1)$–$(2, 1)$, $(2, 0)$–$(3, 0)$, $(2, 1)$–$(3, 1)$ and $(2, 2)$–$(3, 2)$ rotational transitions by using a $\pi, \tau, \pi/2$ pulse sequence method. T_1 relaxation has been investigated for the pure gas and mixtures with He, Ne, Ar, Kr, H_2, O_2, N_2 and CO_2. The effects of molecular motion are discussed theoretically by considering the microwave field inhomogeneity and collisions of molecules with the walls of the sample cell.

I. Introduction

Since the earliest days of microwave spectroscopy the study of rotational energy transfer by gas phase molecular collisions has been of interest. Until recently, most investigations were carried out in the frequency domain and concerned with the pressure dependence of rotational linewidths giving a single parameter (T_2) for the decay of phase coherence between the members of an ensemble of two level systems. In the last few years microwave transient experiments have been developed for the direct observation of rotational relaxation in the time domain [1].

The interpretation of single resonance transient experiments is based on a model which involves the electric dipole interaction of the microwave radiation with an ensemble of two-level systems. The experimental results are interpreted by the appropriate solutions of the differential equations for the induced macroscopic polarization components P_r and P_i and the two level population difference ΔN (Bloch equations) [2].

The information about relaxation processes is contained in the relaxation times T_1 and T_2. T_1 describes the decay of ΔN to its Boltzmann equilibrium value ΔN_0 in the absence of radiation and is related to collisions which change the molecular state. T_2 represents the relaxation time for induced polarization resulting from the superposition of states and is related to phase and state changing collisions.

Reprint requests to Dr. H. Mäder, Abt. Chemische Physik, Institut für Physikalische Chemie der Universität Kiel, Olshausenstr. 40/60, D-2300 Kiel.

We report here on the measurement of T_1 of several M-resolved rotational transitions of OCS by means of a $\pi, \tau, \pi/2$ pulse sequence method [3] which employs the Stark-switching technique to bring the molecular two-level systems into or out of resonance with the microwave radiation. The theory to describe the observed transient phenomena is extended to a consideration of the effects of translational motion of molecules and is outlined in Section II. In Sect. III we report on the experimental results for the pressure and temperature dependence of T_1 for the pure gas and mixtures with He, Ne, Ar, Kr, H_2, O_2, N_2 and CO_2.

II. Theory

A theoretical analysis of the Bloch equations to describe the $\pi, \tau, \pi/2$ pulse sequence experiment has been given previously [3], neglecting the effects of translational motion of molecules. Such approximate treatment may be justified by the fact, that the molecular displacement is usually small with respect to the cell dimensions in the course of the experiment to make microwave field inhomogeneities and collisions with the walls of the sample cell unimportant. To support on this argument somewhat more quantitatively the molecular velocity distribution has been included in the following theoretical derivations.

The times as involved in the pulse sequence are defined analogous to [3]. Each experiment starts at $t = 0$, with the system in its thermodynamical equilibrium conditions ($P_r(0) = P_i(0) = 0$, $\Delta N(0) = \Delta N_0$). An approximate π pulse ($0 \leqq t \leqq t_1$) then creates zero polarization and approximate popula-

0340-4811 / 79 / 1000-1170 $ 01.00/0. — Please order a reprint rather than making your own copy.

Dieses Werk wurde im Jahr 2013 vom Verlag Zeitschrift für Naturforschung in Zusammenarbeit mit der Max-Planck-Gesellschaft zur Förderung der Wissenschaften e.V. digitalisiert und unter folgender Lizenz veröffentlicht: Creative Commons Namensnennung-Keine Bearbeitung 3.0 Deutschland Lizenz.

This work has been digitalized and published in 2013 by Verlag Zeitschrift für Naturforschung in cooperation with the Max Planck Society for the Advancement of Science under a Creative Commons Attribution-NoDerivs 3.0 Germany License.

Zum 01.01.2015 ist eine Anpassung der Lizenzbedingungen (Entfall der Creative Commons Lizenzbedingung „Keine Bearbeitung") beabsichtigt, um eine Nachnutzung auch im Rahmen zukünftiger wissenschaftlicher Nutzungsformen zu ermöglichen.

On 01.01.2015 it is planned to change the License Conditions (the removal of the Creative Commons License condition "no derivative works"). This is to allow reuse in the area of future scientific usage.

tion inversion by the resonant interaction of the two-level systems with the microwave radiation. At times $t > t_1$ the system is taken far out of resonance and the population difference decays back to its equilibrium value with the relaxation time T_1. By bringing the system again into resonance at time $t_2 = t_1 + \tau$, this decay is monitored as a function of delay time τ between the two pulses.

We neglect, for the present, intermolecular collisions and discuss only the effects of translational motion of molecules which — by Doppler broadening, wall collisions and microwave field inhomogeneity — may influence the experimental results. The Doppler-shift of the resonance frequency which is due to velocity components along the direction of microwave propagation affects only the T_2-relaxation in the non-resonance period ($t_1 \leqq t \leqq t_2$) and may be neglected here for the times where the system interacts with the microwave radiation which implies that power broadening is large with respect to Doppler broadening for the transitions of interest.

The collisions of molecules with the walls of the sample cell are believed to the hard collisions which leave molecules in a Boltzmann distribution of states and therefore should contribute equally to the observed decay times for population difference and induced polarization. They are usually not considered explicitely when analyzing transient experiments by assuming that they cause exponential decay behaviour independent of pressure. The approximative nature of this treatment which gives rise to a nonzero intercept for the pressure-versus-inverse relaxation time curves is discussed in detail below.

Finally we will consider the effects of microwave field inhomogeneities in the waveguide cells as used in the experiments to be described here. Molecular motion in nonzero field gradients as present in waveguides may influence the observed T_1 decay curves since the power densities of exciting and monitoring radiation are then no longer identical *.

To solve the Bloch equations for the pulse sequence as defined above, the actual microwave field distribution across the sample must be considered. For the rectangular waveguide with the cross section $a \times b$ (x, y-direction) and length l (z-direction, $l > a > b$) we assume the TE_{10} mode being dominant

$$E(\boldsymbol{r}, t) = 2\,\varepsilon_0 \sin(\pi\, x/a) \cos(\omega\, t - k\, z)\,, \qquad (1)$$

where E is the electric field amplitude along the y-direction depending on position $\boldsymbol{r} = (x, y, z)$ and time t. ω is the microwave angular frequency and $k = \omega/c$ the wave number with c the microwave phase velocity for the mode of consideration. It has been argued [5] that higher modes which might occur in overdimensioned waveguide cells are unimportant for the analysis by using detectors which are adapted to a special frequency range and only sensitive to the ground mode. Weak losses in microwave power density due to wall absorption only negligibly affect the time dependence of the pulse sequence transient signal since the mean free path of molecules is usually small with respect to cell length l. Consequently a term accounting for cell attentuation has been dropped in Equation (1).

For optically thin samples the source radiation, Eq. (1), enters into the Bloch-equations to calculate the time variation of P_r, P_i and ΔN. The resulting macroscopic polarisation of the medium of which the second time derivative represents the source term in the wave equation [2] may excite different modes in the waveguide (see appendix) due to nonlinear absorption (saturation effects). We again consider only its contribution to the ground mode (TE_{10}) by using the arguments as given above. Then, as shown in the appendix, for a general solution of the form

$$P(\boldsymbol{r}, t) = 2\,P_r(\boldsymbol{r}, t) \cos(\omega\, t - k\, z) - 2\,P_i(\boldsymbol{r}, t) \sin(\omega\, t - k\, z) \qquad (2)$$

the observed change of signal at the output of a square law diode detector $\Delta S(t)$ is related to the polarization component P_i which is in quadrature to the field (1)

$$\Delta S(t) = (8\pi\,\beta\,\omega\, l/c_g)\,\varepsilon_0\,\tilde{P}_i(t)\,. \qquad (3)$$

β is a constant, characterizing the diode efficiency, c_g the microwave group velocity and $\tilde{P}_i(t)$ is given by

$$\tilde{P}_i(t) = (2/a)(1/b)(1/l) \cdot \int_0^a a\,\mathrm{d}x \sin(\pi\, x/a) \int_0^b b\,\mathrm{d}y \int_0^l l\,\mathrm{d}z\, P_i(\boldsymbol{r}, t)\,. \qquad (4)$$

* In a similar way the translational motion of molecules in a nonuniform microwave field distribution had to be included to describe theoretically the formation and damping of rotary photon echos [4].

We now proceed and discuss the solutions of the Bloch equations for the pulse sequence. At times $0 \leqq t \leqq t_1$ the mean displacement of molecules is small compared to the cell dimensions ($\lesssim 3 \cdot 10^{-2}$ cm for $t \lesssim 1$ μsec, see experimental conditions Sect. III) and we neglect, to simplify the following discussion, the translational motion in that period of time. Then the resonant solutions of the Bloch-equations are given by [3]

$$\begin{aligned} P_r(\boldsymbol{r}, t) &= 0\,, \\ P_i(\boldsymbol{r}, t) &= -(\hbar \varkappa \Delta N_0/4) \sin(\varkappa \varepsilon_0 t) \sin(\pi x/a))\,, \quad (5) \\ \Delta N(\boldsymbol{r}, t) &= \Delta N_0 \cos(\varkappa \varepsilon_0 t \sin(\pi x/a)) \end{aligned}$$

for $0 \leqq t \leqq t_1$. $\varkappa$ is proportional to the transition dipole matrix element, $\varkappa = 2|\mu_{ab}|/\hbar$.

With (3), (4) and (5) we obtain for the observed change in signal

$$\Delta S(t) = -(4\pi \beta \omega l/c_g) \hbar \varkappa \Delta N_0 \varepsilon_0 J_1(\varkappa \varepsilon_0 t) \quad (6)$$

where J_1 is the first order Bessel function.

The condition $\Delta S(t_1) = 0$ defines the end of the π-pulse when maximum change of average population difference has been achieved [3]. Then the system is brought out of resonance with the radiation field. If $\boldsymbol{r}_0$ defines the position of a macroscopically small ensemble of molecules at time $t = t_1$, moving with velocity $\boldsymbol{v}$ the position at time $t > t_1$ will be at $\boldsymbol{r} = \boldsymbol{r}_0 + \boldsymbol{v}(t - t_1)$ in the absence of collisions. We then obtain with the initial conditions (5) at $\boldsymbol{r} = \boldsymbol{r}_0$ for one velocity group $\boldsymbol{v}(v_x v_y v_z)$ at $t_2 = t_1 + \tau$, omitting P_r which does not contribute to the observed signal

$$\begin{aligned} P_i(\boldsymbol{r}, t_2; \boldsymbol{v}) &= -(\hbar \varkappa \Delta N_0/4) \\ &\quad \cdot \sin(\varkappa \varepsilon_0 t_1 \sin(\pi(x - v_x \tau)/a)) \cos \Delta\omega' \tau\,, \\ \Delta N(\boldsymbol{r}, t_2; \boldsymbol{v}) - \Delta N_0 &= \Delta N_0 \{\cos(\varkappa \varepsilon_0 t_1 \sin(\pi(x - v_x \tau)/a)) - 1\} \quad (7) \end{aligned}$$

where $\Delta\omega' = \Delta\omega + (\omega v_z/c)$, with $\Delta\omega = \omega_0 - \omega$, is the Doppler-shifted offset from resonance frequency as achieved by Stark-switching.

Only those molecules which have not yet collided with the walls of the sample cell at time t_2 will contribute to non-zero solutions (7). The range of velocities over which we have to integrate Eqs. (7) is finite and depends on position $\boldsymbol{r}(x, y, z)$ and time τ which introduces additional time dependence into the solution. Since the initial position is restricted to be within the waveguide, we have

$$\begin{aligned} &0 \leqq x - v_x \tau \leqq a, \quad 0 \leqq y - v_y \tau \leqq b\,, \\ &0 \leqq z - v_z \tau \leqq 1 \quad (8) \end{aligned}$$

which gives the limits for the $\boldsymbol{v}$-integration

$$\begin{aligned} &(x - a)/\tau \leqq v_x \leqq x/\tau, \quad (y - b)/\tau \leqq v_y \leqq y/\tau, \\ &(z - l)/\tau \leqq v_z \leqq z/\tau\,. \quad (9) \end{aligned}$$

Then, if the velocity distribution is assumed to be Maxwellian, we have the velocity-averaged solutions at $t_2 = t_1 + \tau$

$$\begin{aligned} P_i(\boldsymbol{r}, t_2) &= \iiint \mathrm{d}v_x\, \mathrm{d}v_y\, \mathrm{d}v_z\, W(v_x, v_y, v_z)\, P_i(\boldsymbol{r}, t_2; \boldsymbol{v})\,, \\ \Delta N(\boldsymbol{r}, t_2) - \Delta N_0 &= \iiint \mathrm{d}v_x\, \mathrm{d}v_y\, \mathrm{d}v_z\, W(v_x, v_y, v_z) \\ &\quad \cdot (\Delta N(\boldsymbol{r}, t_2; \boldsymbol{v}) - \Delta N_0)\,. \quad (10) \end{aligned}$$

The integration is carried out over the range given by (9) and

$$\begin{aligned} &W(v_x, v_y, v_z) \quad (11) \\ &\quad = (\pi v_0^2)^{-3/2} \exp\{-(v_x^2 + v_y^2 + v_z^2)/v_0^2\}\,, \end{aligned}$$

where v_0 is the most probable velocity, $v_0 = \sqrt{2kT/m}$, with m the molecular mass, T the temperature and k Boltzmann's constant.

In the following, we consider for further simplification only the collision with the walls along the shortest cell dimension ($y = 0$ and $y = b$) by extending the integration limits of v_x and v_y to infinity as may be justified to good approximation for the type of waveguide cells used in the experiment ($b : a : l \cong 1 : 10 : 600$, see Sect. III) and the short times involved in the sequence ($v_0 \tau \ll a, l$). By using the latter condition, we may develop the solution (7) to first order with respect to $(\pi v_x \tau/a)$ and obtain, carrying out the integration of (10)

$$\begin{aligned} P_i(\boldsymbol{r}, t_2) &= -(\hbar \varkappa \Delta N_0/4) \sin(\varkappa \varepsilon_0 t_1 \sin(\pi x/a)) \\ &\quad \cdot \exp\{-\tfrac{1}{4}(\omega v_0/c)^2 \tau^2\} f(x, \tau)\, g(y, \tau) \cos \Delta\omega \tau\,, \\ \Delta N(\boldsymbol{r}, t_2) - \Delta N_0 &\quad (12) \\ &= \Delta N_0 [\cos(\varkappa \varepsilon_0 t_1 \sin(\pi x/a)) f(x, \tau) - 1]\, g(y, \tau)\,, \end{aligned}$$

where

$$f(x, \tau) = \exp\{-\tfrac{1}{4}(\varkappa \varepsilon_0 t_1 \pi v_0 \cos(\pi x/a)^2 \tau^2\}\,, \quad (13)$$

accounts for molecular motion along the field inhomogeneity in x-direction, and

$$g(y, \tau) = \frac{1}{2} \operatorname{erf}\left(\frac{y}{v_0 \tau}\right) + \operatorname{erf}\left(\frac{b - y}{v_0 \tau}\right) \quad (14)$$

is due to wall collisions. $\operatorname{erf}(\xi)$ denotes the error-function defined by

$$\operatorname{erf}(\xi) = \frac{2}{\sqrt{\pi}} \int_0^{\xi} e^{-\xi'^2}\, \mathrm{d}\xi'\,. \quad (15)$$

The Doppler-term $\exp\{-\frac{1}{4}(\omega v_0/c)^2\tau^2\}$ contributes only to the solution for P_i.

So far, we have not considered the intermolecular collisions which, of course, give a dominant contribution to the time dependencies of transient experiments. The bulk quantities T_1 and T_2 which are introduced phenomenologically into the Bloch equations are averages over various collision parameters such as impact parameter, state of perturber molecule and relative velocities of collision partners. We account for these collisional effects by simply multiplying the solutions (12) for P_i and $\Delta N - \Delta N_0$ with $\exp(-\tau/T_2)$ and $\exp(-\tau/T_1)$ respectively.

Such procedure ignores the effects of velocity-changing, elastic collisions which do not contribute to T_1. Obviously such collisions are also unimportant in contributing to T_2 since $T_1 \approx T_2$ for the considered transitions, see discussions below in this article. We neglect here the effects of elastic collisions which change only the velocity of molecules. The decay behaviour of infrared photon echos, observed on methyl fluoride [6], suggests that such „velocity-diffusion" is predominantly due to small velocity jumps (< 1 m/sec) through small angle scattering. This result supports the above approximate treatment which considers the molecules to move along a linear path even if they have suffered collisions which do not contribute to T_1 and T_2.

We now have with the initial conditions (12) and inclusion of molecular relaxation (T_1, T_2) at times $t > t_2$ when the system is again in resonance with the radiation field [2] (neglecting motional effects as discussed before)

$$\begin{aligned} P_i(\boldsymbol{r}, t; \tau \to \infty) - P_i(\boldsymbol{r}, t; \tau) = &- (\hbar \varkappa \Delta N_0/4)\big[\{1 - \cos(\varkappa \varepsilon_0 t_1 \sin(\pi x/a))f(x,\tau)\} \\ &\cdot e^{-\tau/T_1} \sin(\varkappa \varepsilon_0 (t - t_2) \sin(\pi x/a)) - \sin(\varkappa \varepsilon_0 t_1 \sin(\pi x/a)) \\ &\cdot \exp\{-\tfrac{1}{4}(\omega v_0/c^2 \tau^2\} f(x,\tau) \\ &\cdot e^{-\tau/T_2} \cos \Delta\omega \tau \cos(\varkappa \varepsilon_0 (t - t_2) \sin(\pi x/a))\big] g(y,\tau)\,. \end{aligned} \tag{16}$$

Equation (16) gives the difference of polarization component P_i to the solution for $\tau \to \infty$ and is related to the observed difference in signal by means of Eqs. (3) and (4). To carry out the integration (4) we may develop $f(x,\tau)$ (13) to first order, as $(\varkappa \varepsilon_0 t_1 \pi v_0 \tau/2a) \ll 1$

$$f(x,\tau) \approx 1 - (\varkappa \varepsilon_0 t_1 \pi v_0 \tau/2a)^2 \cos^2(\pi x/a)\,. \tag{17}$$

With Eqs. (3), (4), (14), (15)*, (16) and (17) we then have, for convenience defining $t' = t - t_2$

$$\begin{aligned} \Delta S(t';\tau \to \infty) - \Delta S(t';\tau) = &- (2\pi \beta \omega \hbar \varkappa \Delta N_0 \varepsilon_0 l/c_g) \\ &\cdot\big[\{2J_1(\varkappa \varepsilon_0 t') - J_1(\varkappa \varepsilon_0 (t_1 + t')) + J_1(\varkappa \varepsilon_0 (t_1 - t')) + (\varkappa \varepsilon_0 t_1 \pi v_0/4a)^2 \tau^2 \\ &\cdot [J_1(\varkappa \varepsilon_0 (t_1 + t')) + J_3(\varkappa \varepsilon_0 (t_1 + t')) - J_1(\varkappa \varepsilon_0 (t_1 - t')) - J_3(\varkappa \varepsilon_0 (t_1 - t'))]\} e^{-\tau/T_1} \\ &- \{J_1(\varkappa \varepsilon_0 (t_1 + t')) + J_1(\varkappa \varepsilon_0 (t_1 - t')) - (\varkappa \varepsilon_0 t_1 \pi v_0/4a)^2 \tau^2 [J_1(\varkappa \varepsilon_0 (t_1 + t')) \\ &+ J_3(\varkappa \varepsilon_0 (t_1 + t')) + J_1(\varkappa \varepsilon_0 (t_1 - t')) + J_3(\varkappa \varepsilon_0 (t_1 - t'))]\} \exp\{-\tfrac{1}{4}(\omega v_0/c)^2 \tau^2\} \\ &\cdot e^{-\tau/T_2} \cos \Delta\omega \tau\big] g_w(\tau). \end{aligned} \tag{18}$$

J_3 is the third order Bessel function and $g_w(\tau)$ accounts for wall collisions

$$\begin{aligned} g_w(\tau) = 1 &- (v_0 \tau/\sqrt{\pi}\, b) \\ &\cdot (1 - \exp\{-(b/v_0 \tau)^2\}) - \operatorname{erf} c\,(b/v_0 \tau)\,, \end{aligned} \tag{19}$$

where $\operatorname{erf} c = 1 - \operatorname{erf}$ is the error-cofunction.

We now discuss the solution (18) for the experimental conditions at time t' which gives maximum change in signal $\Delta S(t';\tau \to \infty)$, that is [3]

$$\varkappa \varepsilon_0 t' \approx 1.84\,. \tag{20}$$

* The integral for $g(y,\tau)$ is most easily solved by interchanging the integration order with respect to y und v_y.

Using Eq. (6) with $\Delta S(t_1) = 0$ defines the length of the first near π-pulse [3]

$$\varkappa \varepsilon_0 t_1 \approx 3.83\,. \tag{21}$$

Then, with (18), (20) and (21) we have

$$\begin{aligned} \Delta S(t';\tau \to \infty) - \Delta S(t';\tau) &= - (2\pi \beta \omega \hbar \varkappa \Delta N_0 \varepsilon_0 l/c_g) \\ &\cdot [2.07\{1 - 3.59(v_0 \tau/a)^2\} e^{-\tau/T_1} \\ &- 0.25\{1 - 21.28(v_0 \tau/a)^2\} \\ &\cdot \exp\{-\tfrac{1}{4}(\omega v_0/c)^2 \tau^2\} e^{-\tau/T_2} \cos \Delta\omega \tau]\, g_w(\tau). \end{aligned} \tag{22}$$

With neglection of molecular motion ($v_0 = 0$)

Eqs. (18) and (22) are in agreement with the solutions (36) and (38) of [3].

The contribution of T_2 in Eq. (22) which disappears for $\Delta\omega\tau = \frac{1}{2}n\pi$ ($n = 1, 3, 5, \ldots$) is general small and will be neglected in the following**. This neglection may be partly justified by the different amplitude factors in Eq. (22) and the faster decay of polarization due to inhomogeneous Doppler-broadening, corresponding to the term

$$\exp\{-\tfrac{1}{4}(\omega v_0/c)^2\tau^2\}$$

in Equation (22). An additional important dephasing mechanism which has not been considered so far, results from the experimental condition of nonzero Stark-field during the delay period τ (see Section III). The Stark-field inhomogeneity which leads to spatial incoherence and thereby strongly damps the T_2 decaying oscillations, does not contribute to T_1.

For further analysis of Eq. (22) we make use of the approximation [7]

$$\operatorname{erf} c(b/v_0\tau) \approx (1/\sqrt{\pi})(v_0\tau/b)\exp\{-(b/v_0\tau)^2\} \quad (23)$$

for $b/v_0\tau \gg 1$ which gives with Eq. (19)

$$g_w(\tau) \approx 1 - (v_0\tau/\sqrt{\pi}\, b)\,. \quad (24)$$

The accuracy of Eq. (24) may be shown to be better than 0.2% for $\tau < 40$ μsec ($b \cong 0.5$ cm, $v_0 \cong 2.5\times 10^4$ cm/sec) which gives the typical range of delay times as used for the analysis of the pulse sequences (see Section III).

Then, with (24) and neglecting T_2 contributions as discussed before, we rewrite Eq. (22)

$$\Delta S(t';\tau\to\infty) - \Delta S(t';\tau) \quad (25)$$
$$= -C[1 - 3.59(v_0\tau/a)^2][1 - (v_0\tau/\sqrt{\pi}\, b)]\, e^{-\tau/T_1}$$

where $C = 2.07(2\pi\beta\omega\hbar\varkappa\Delta N_0\varepsilon_0 l/c_g)$ includes all terms which do not depend on τ.

Equation (25) exhibits nonexponential decay behaviour due to microwave field inhomogeneity and wall collisions which was not observed experimentally for the range of investigated pressure. The experimental uncertainties, as discussed in detail in Sect. III, are too large to allow for detection of these small effects which are more important at longer delay times where the signal-to-noise ratio is poor. For shorter delay times ($\lesssim 20$ μsec) and $a \gg b$ we may neglect the inhomogeneity term $(v_0\tau/a)^2$ with respect to unity ($3.59(v_0\tau/a)^2 \lesssim 0.01$ for $a = 5$ cm) and replace $g_w(\tau)$, Eq. (24), by an exponential function*

$$g_w(\tau) \approx \exp\{-(v_0\tau/\sqrt{\pi}\, b)\}\,. \quad (26)$$

Using Eq. (26) we may rewrite Eq. (25) in terms of a single damping constant T_1'

$$\Delta S(t';\tau\to\infty) - \Delta S(t';\tau) = C\, e^{-\tau/T_1'} \quad (27)$$

where

$$1/T_1' = 1/T_1 + v_0/\sqrt{\pi}\, b\,. \quad (28)$$

The data analysis is based on Eq. (27), see following section. The experiments, within its error limits confirm the magnitude of zero pressure intercept for the pressure dependence of $1/T_1'$ predicted to be $(v_0/\sqrt{\pi}\, b)$ by Equation (28).

III. Experimental and Results

The apparatus which was used for the experiments is based on a conventional MW-Stark spectrometer and has been described in detail recently for the investigation of transient emission signals [8]. Only the modifications for the π, τ, $\pi/2$ pulse sequence experiments are reported here. The microwave radiation which was fed into the Stark cell (inner dimensions $1\times 4.7\times 340$ cm) was supplied from phase stabilized MW-sources which were BWO's in the X- and K-band and a OKI 35V12 Klystron in the V-band.

To minimize reflections ferrite isolators were inserted in front of the detectors. Since only a single-point information of the broadband amplified transient signal is essentially needed to analyze the T_1-relaxation in the π, τ, $\pi/2$ pulse sequence, see Eqs. (20) and (27), the Boxcar integrator is the most suited instrument for this type of experiment. In single-point analysis the integrators aperture position is held fixed with respect to a trigger signal.

To control the pulse sequence experiment a unit was constructed which delivered pairs of pulses at TTL-level, each variable in length (0.3 to 2 μsec).

** Remaining small terms in T_2 may be averaged out from the oscillating decay behaviour of the signal, see discussion in Ref. [3].

* Accounting for wall collisions by using kinetic-theory arguments [23] results in approximation (26). Such treatment allows for multiple collisions with the walls of the sample cell and does not consider explicitely the molecular velocity distribution which gives generally rise to non-exponential decay behaviour, see text.

Starting with an adjustable minimum delay time, the delay between the pulses was increased in steps of 100 nsec as determined by control of a quarz ossillator. For a fixed delay time the two-pulse sequence was repeated for a preselected number of times with a repetion rate of about 1.5 kHz. The pulses were amplified by the Stark generator up to 450 Volt to satisfy the conditions for on-off-resonance Stark-switching. A TTL-level output pulse which was synchronized to the second pulse of the pair served as trigger for the Boxcar integrator which was driven in single-point analysis mode. The aperture position was adjusted to give maximum signal at long delay times corresponding to times t', see Eq. (20), and remains fixed in the course of the experiment. Due to synchronisation, always the same portion of the absorption signal is probed and averaged, independent of delay time τ. Thus, the decay of approximate population inversion as achieved by the first pulse is observed directly at the Boxcar integrators analog output which, for further averaging, was A/D converted and digitally averaged for repeated experiments. The trigger pulses for the memory adress advance of the digital averager (Fabri-Tek Mod. 1072) were supplied by the control unit synchroniously to delay time switching. For further analysis the data were transferred to a PDP-11 computer.

The OCS sample used in the experiments after distillation was analyzed by gas chromatography. The impurity of 0.3% CO_2 which was found is thought to be insignificant. The sample pressure was varied from about 6 to 35 mTorr for the pure gas. The partial pressures for the foreign gases (He, Ne, Ar, Kr, H_2, O_2, N_2 and CO_2) were in the range of 0 to 50 mTorr. For details of partial pressure determination see [3].

The experiments were carried out at room temperature ($\simeq$300 K) and 200 K.

The T_1-relaxation has been investigated for the rotational transitions $(J, |M|)$:

$$(0,0)\text{–}(1,0),\quad (1,0)\text{–}(2,0),\quad (1,1)\text{–}(2,1),$$
$$(2,0)\text{–}(3,0),\quad (2,1)\text{–}(3,1)\ \text{and}\ (2,2)\text{–}(3,2)$$

of the OCS normal species in the ground vibrational state. Stark pulses of 200 volt for the $J=0$–1, 1–2 transitions and 400 volt for the $J=2$–3 transitions, respectively, were applied to bring the transition of interest into resonance with the microwave radiation field. An additional DC Stark voltage was used to shift the $|M|$ transitions several MHz from zero field transition frequency during the nonresonant delay period between the pulses, ranging from 400 volt for the $J=0$–1 transition to 3100 volt for the $J, |M|=(2,1)$–$(3,1)$ transition. For the investigation of the latter transition the Stark bias is indispensable in order to avoid polarization of the $J, |M|=(2,0)$–$(3,0)$ transition due to fast passage [9]. A general additional advantage results from the fact that the residual polarization** after the first π pulse decays appreciable faster in the presence of an inhomogeneous Stark field, see discussion above.

The observed signal behaviour is demonstrated in Fig. 1 for the $(J, M)=(0,0)$–$(1,0)$ transition at 9 mTorr pressure and 200 K temperature. The pressure dependence of $1/T_1$ was obtained by performing two least squares fitting procedures in sequence. At first the expression

$$\Delta S(x) = A\, e^{-Bx} + C \tag{29}$$

was used in the least squares analysis of the data points stored in the PDP-11 computer with A, B and C as fitting parameters. Equation (29) corresponds to the theoretical expression for $\Delta S(t';\tau)$, Eq. (27), with arbitrary offset. A data point internal Δx corresponds to a 100 nsec time interval in delay time τ.

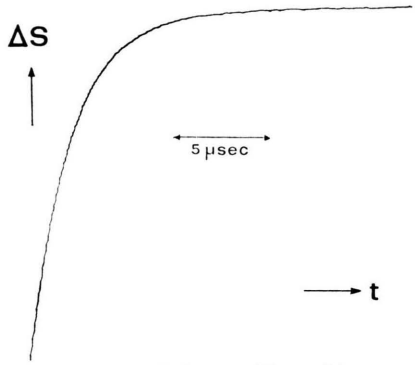

Fig. 1. Observed change ΔS in arbitrary units of the Boxcar Integrator output corresponding to the second pulse absorption in dependence of the delay time between the two pulses. OCS $(J, M) = (0,0)$–$(1,0)$ transition, $p =$ 9 mTorr, $T = 200$ K.

** Even for zero signal during the nonresonant delay period between the two pulses nonzero polarization exists due to microwave field inhomogeneity [3]. The influence of its component P_i to the second pulse period solution is evident for Eqs. (16), (18) and (22) by the term involving the relaxation time T_2.

Table 1. Slope (β) and intercept (α) from the least squares analysis of the plots of $1/T_1$ against pressure of OCS.

Transition $J-J', \lvert M \rvert$	T [K]	Slope (β) [μsec^{-1} mTorr^{-1}]	Intercept (α) [μsec^{-1}]
0—1, 0	304[b]	0.0381 (5)[a]	0.043 (4)
	200	0.0507 (7)	0.029 (6)
1—2, 0	298	0.0381 (10)	0.041 (8)
	200	0.0505 (13)	0.018 (8)
1—2, 1	298	0.0359 (4)	0.049 (4)
	200	0.0482 (8)	0.028 (5)
2—3, 0	295	0.0382 (15)	0.042 (12)
	200	0.0474 (8)	0.039 (6)
2—3, 1	297	0.0372 (25)	0.051 (12)
	200	0.0467 (34)	0.036 (12)
2—3, 2	297	0.0368 (8)	0.047 (6)
	200	0.0470 (7)	0.034 (6)

[a] Errors in parantheses are in the last digit given and twice the standard deviations.

[b] Temperature uncertainties ± 1 K at room temperature, and ± 3 K at 200 K.

From the results for $1/T_1$ and its standard errors at different sample pressures the coefficients for the linear pressure dependence are then evaluated by using a linear least squares fit and weighting the $1/T_1$ data points with their standard deviations. The resulting intercepts (α) and slopes (β) for the pure gas are given in Table 1. For the mixtures the dependence of $1/T_1$ on the foreign gas partial pressure (p_{fg}) is linear in the binary collision approximation, $1/T_1 = \alpha + \beta p_{OCS} + \gamma p_{fg}$. Only the slope coefficients γ are given in Table 2. The intercept values depend on the initial partial pressure of OCS which was in the range from 5 to 10 mTorr.

The error limits which are given in Table 1 and 2 for intercept (α) and slope (β and γ) do not reflect systematic deviations which are primarily due to shifts in pressure (< 0.1 mTorr) and temperature (< 3 K). These inaccuracies of the experimental conditions lead to an additional error of the intercept ($\sim 4 \cdot 10^{-3}$ μsec^{-1}) and the slope ($\sim 3 \cdot 10^{-4}$ μsec^{-1} mTorr^{-1}) for the pure gas measurements.

For the mixtures an additional error ($< 5\%$) may result from partial pressure inaccuracies.

Several variations of the experimental conditions were carried out to check on the reproducibility of the results. No significant dependence of the T_1 value on the Stark bias voltage was observed. For the applied microwave power (~ 10 mW) Stark switching of about 3 MHz was found to be sufficient to make off-resonant transient absorption effects during the delay period unimportant. For the $(J, \lvert M \rvert) = (2, 1)$–$(3, 1)$ transition a lower microwave power was used (~ 1 mW) since the change in transition frequency was only about 1 MHz for the applied Stark voltages (3100—3500 volt). Higher voltages were causing a discharge* in the

* Due to discharge effects only a few mixture measurements were made for the $(J, \lvert M \rvert) = (2, 1)$–$(3, 1)$ transition, see Table 2.

Table 2. Slopes (γ) from the least squares analysis of the plots of $1/T_1$ against the pressure of He, Ne, Ar, Kr, H_2, O_2, N_2, and CO_2.

Transition $J-J', \lvert M \rvert$	T [K]	Slope (γ) [μsec^{-1} mTorr^{-1}] for Foreign Gases							
		He	Ne	Ar	Kr	H_2	O_2	N_2	CO_2
0—1, 0	R.T.[b]	0.0214 (6)[a]	0.0188 (5)	0.0240 (5)	0.0220 (5)	0.0401 (5)	0.0243(10)	0.0285 (3)	0.0346 (5)
	200	0.0279 (4)	0.0236 (3)	0.0292 (7)	0.0293(10)	0.0526 (5)	0.0317 (5)	0.0359 (5)	0.0464 (8)
1—2, 0	R.T.	0.0216(10)	0.0175 (8)	0.0232 (6)	0.0213 (8)	0.0389(16)	0.0242(10)	0.0274 (9)	0.0341(24)
	200	0.0278 (5)	0.0243(14)	0.0295 (7)	0.0269(10)	0.0527(24)	0.0315(14)	0.0362 (8)	0.0428(18)
1—2, 1	R.T.	0.0209 (6)	0.0178 (6)	0.0226 (4)	0.0213 (5)	0.0390 (8)	0.0239 (7)	0.0274 (6)	0.0333(13)
	200	0.0269 (4)	0.0236 (7)	0.0291 (7)	0.0272 (7)	0.0519 (7)	0.0316 (5)	0.0349(14)	0.0433(17)
2—3, 0	R.T.	0.0209(11)	0.0164(12)	0.0214(22)	0.0201(13)	0.0392(20)	0.0234(20)	0.0270(24)	0.0300(24)
	200	0.0266(11)	0.0232 (9)	0.0292(13)	0.0256(18)	0.0519(14)	0.0305(14)	0.0344(14)	0.0413(12)
2—3, 1	R.T.	0.0196(12)	—	—	—	—	—	—	—
	200	0.0252(32)	0.0211(32)	0.0238(24)	—	—	—	—	—
2—3, 2	R.T.	0.0220(11)	0.0174(12)	0.0221(13)	0.0211(16)	0.0388(19)	0.0223(19)	0.0261(14)	0.0307(20)
	200	0.0261 (8)	0.0241 (5)	0.0269(12)	0.0267 (6)	0.0501(13)	0.0302(10)	0.0351(12)	0.0433(11)

[a] Errors in parantheses are in the last digit given and twice the standard deviations.

[b] Room temperatures (R.T.) in the range from 296 K to 302 K.

sample cell. As a consequence of a lower power the range of investigated pressures was restricted ($p < 6$ mTorr) to satisfy the „π-pulse" condition $\Delta S(t_1) = 0$ which implies $\varkappa \varepsilon T_1 > 3.7$ [3]. The limited pressure range gives rise to larger error limits of the results (see Tables 1 and 2).

The minimum delay between the two pulses was in general above 2 μsec to minimize effects from residual polarization and a delay dependent small variations of the second Stark pulse amplitude which was found to be more important for larger Stark bias voltages. No significant difference in the results for the pressure dependence of $1/T_1$ was found by increasing the minimum delay time.

A final remark has to be made about the approximative nature of data analysis, based on the exponential form of Equation (29). Though non-exponential decay behaviour as predicted by Eq. (25) has not been detected due to limited sensitivity, approximation (26) will introduce a pressure dependent shift in the results which may be important for the analysis of the pressure dependence of $1/T_1$. To get an estimate of the magnitude of such effect data were simulated numerically according to Eq. (25) for the type of cell and range of pressures (or relaxation times) used in the experiments. The numerical analysis of the simulated data was carried out identical to the real data analysis by the two successive least squares procedures as discussed before. The resulting pressure coefficients (β, γ) are found to be slightly increased with respect to the values which were originally assumed to account for intermolecular collisions in data simulation ($1/T_1$ being proportional to pressure). For the typical range of investigated pressures (> 5 mTorr) the changes in results due to nonexponential relaxation are small ($< 1\%$).

IV. Discussion

The zero pressure intercepts which account for wall collisions are predicted by means of Eq. (28) to be about 0.035 μsec^{-1} and 0.028 μsec^{-1} for $T = 300$ K and 200 K, respectively *. With inclusion of systematic errors as discussed before these values are in reasonable agreement with the results given in Table 1.

For the $J = 0$–1 transition the $1/T_1$ intercept is found to agree within its error limits with the $1/T_2$ intercept from transient emission investigations (unpublished results). This result is in contrast to the work of Coy [10], who found a significantly larger intercept for the pressure dependence of $1/T_1$. Equal intercepts for $1/T_1$ and $1/T_2$ were also found by Hoke et al. [11].

As seen from the results of Tables 1 and 2 the $|M|$ dependence of the $1/T_1$ slope values β and γ is small and mainly hidden in the experimental uncertainties. The difference in the results for the two M components ($0, \pm 1$) of the pure gas $J = 1$–2 transition is thought to be significant since the measurements were carried out alternately at the same time to minimize effects of systematic shifts in the experimental conditions. This results indicates longer T_1 relaxation time for the $M = \pm 1$ components of this transition due to OCS self collisions.

The observed M-dependence of T_1 may be attributed to important contributions from collisions which transfer molecules within the $M = \pm 1$ substates without changing the rotational quantum number J. Such $\Delta J = 0$, $\Delta M = \pm 2$ quadrupole-type collisions would not contribute to the observed T_1 decay behaviour of the $|M| = 1$ transition since the experiment probes the sum of the population difference of both $M = \pm 1$ components which are degenerate in the Stark field. A similar behaviour of increase in relaxation time T_1 of the $|M| = 1$ component of the $J = 2$–3 transition may be obscured by the larger error limits. No detailed theory has been worked out to extend the above qualitative arguments and to relate the observed small M dependence of T_1 to molecular collision dynamics. A more distinct M dependence of T_1 was found for ammonia inversion lines with $1/T_1$ strongly increasing with $|M|$ [15], different from the present conclusions for OCS. This result was predicted correctly by a first-order modified Anderson theory [15] and is primarily due to dipolar collisional transitions which transfer molecules between the probed levels. For OCS such collisions which contribute twice to T_1 relative to T_2 are believed to be unimportant since OCS has many closely spaced rotational energy levels and a small dipole moment. It then follows $T_1 \approx T_2$ if phase

* With $b = 0.47$ cm taken from Stark effect measurements; collisions with other walls which might slightly increase ($< 10\%$) the above given values are not considered.

Table 3. Comparison of experimental results at room temperature for relaxation times T_1 anp T_2 of OCS rotational transitions.

Transition $J-J'$, $\lvert M \rvert$	Slope (β) $1/T_1$	[μsec^{-1} · mTorr^{-1}] $1/T_2$	Method	Ref.
0−1, 0	0.0381 (4)[a]		π, τ, $\pi/2$	[10]
	0.0370 (40)		π, τ, $\pi/2$	[3, 11]
	0.0381 (5)		π, τ, $\pi/2$	this work
		0.0377 (2)	transient emission	[10]
1−2, 0	0.0381 (10)		π, τ, $\pi/2$	this work
		0.0369 (54)	transient emission	[12]
1−2, 1	0.0350 (40)		π, τ, $\pi/2$	[11]
	0.0359 (4)		π, τ, $\pi/2$	this work
		0.0366 (54)	transient emission	[12]
2−3, 0	0.0382 (15)		π, τ, $\pi/2$	this work
1	0.0372 (25)		π, τ, $\pi/2$	this work
2	0.0368 (8)		π, τ, $\pi/2$	this work
0, 1, 2[b]		0.0364 (14)	linewidth	[13]
		0.0358 (16)	linewidth	[14]

[a] Errors in paranthesis are in the last digit given and twice the standard deviations.
[b] M-components not resolved in linewidth studies.

changing collisions which contribute only to T_2 are unimportant.

The above conclusion is strongly supported by the experimental results given in Table 3 which compares values for the pressure dependence of $1/T_1$ and $1/T_2$ as obtained by various methods in different laboratories. Within the given uncertainties one finds $T_1 = T_2$ for the investigated transitions.

Only little work has been done so far on the investigation of T_1 relaxation in mixtures with foreign gases. The value $\gamma = 0.020 \pm 0.002$ μsec^{-1} · mTorr^{-1} which was given previously for the OCS $J = 0$–1, $M = 0$ transition in mixtures with He [3] is in agreement with the result of this work. The mixture measurements should be useful to check the reliability of recent theoretical approaches to collision dynamics for the determination of microwave relaxation rates [16a, b, c], [17a, b], [18]. T_1 relaxation cross sections which were calculated for OCS-He and OCS-Ar collisions by Liu et al. [16b] and by Green [18] are compared in Table 4 with the experimental results of this paper.

Table 4. Comparison of calculated and measured cross sections for T_1 at $T \cong 300$ K. For definition of $\sigma(T_1)$ see [16].

Transition $J-J'$, $\lvert M \rvert$		$\sigma(T_1)$ [Å^2] (calculated) Ref. [16]	Ref. [18]	$\sigma(T_1)$ [Å^2] (measured) this work
0−1, 0	OCS-He	36	33	51
	OCS-Ar	146	145	145
1−2, 0	OCS-He	38	32	52
	OCS-Ar	141	144	139
1−2, 1	OCS-He	34	29	50
	OCS-Ar	138	140	135

Good agreement to the theoretical results is obtained for the OCS-Ar mixtures. A systematic discrepancy is found for the mixtures with He.

T_1 relaxation rates are related to the transfer of rotational energy due to molecular collisions and thereby to the rate constants describing the transfer of energy level population probabilities [19]. Additional information on collisional transition probabilities is obtained from four-level double resonance investigation of collision-induced transitions.

The description and results of microwave-microwave-double resonance (MWMWDR) experiments for the investigation of collisional energy transfer in OCS pure gas and mixtures with nonpolar foreign gases will be the subject of a forthcoming paper.

Appendix

Equations (3) and (4) are derived by developping the polarisation components P_r and P_i in Eq. (2) in normal mode eigenfunctions TE_{nm} (y-component)

$$P_g(\boldsymbol{r}, t) = \sum_{\substack{n=1 \\ m=0}} P_g{}^{nm}(z, t) \sin(n\pi x/a) \cdot \cos(m\pi y/b), \quad g = r, i \tag{A.1}$$

and retaining only the terms

$$P_g{}^{10}(z, t) = (2/a)(1/b) \int_0^a \mathrm{d}x \sin(\pi x/a) \cdot \int_0^b \mathrm{d}y \, P_g(\boldsymbol{r}, t), \quad g = r, i \tag{A.2}$$

as source for the TE_{10}-mode in the wave equation.

Then with the trial solution*

$$\tilde{E}(\boldsymbol{r}, t) = 2\sin(\pi x/a)[\varepsilon_r(z,t)\cos(\omega t - k z) - \varepsilon_i(z,t)\sin(\omega t - k z)] \quad (A.3)$$

for the field in the sample, the wave equation may be reduced under the slowly varying enveloppe assumption for P_r, P_i, ε_r and ε_i [21] to the following equations for ε_r and ε_i

$$\frac{\partial \varepsilon_r}{\partial z} + \frac{1}{c_g}\frac{\partial \varepsilon_r}{\partial t} = \frac{2\pi\omega}{c_g} P_i^{10},$$
$$\frac{\partial \varepsilon_i}{\partial z} + \frac{1}{c_g}\frac{\partial \varepsilon_i}{\partial t} = -\frac{2\pi\omega}{c_g} P_r^{10}. \quad (A.4)$$

To derive Eqs. (A.4) use has been made of the relation $(\pi/a)^2 + k^2 - k_0^2 = 0$ for the TE_{10}-mode [22] where $k_0 = \omega/c_0$ is the free space wave number with c_0 the vacuum light velocity. The product of microwave velocity and group velocity is constant, $c \cdot c_g = c_0^2$ [22].

Neglecting the terms

$$(1/c_g)(\partial\varepsilon_r/\partial t) \quad \text{and} \quad (1/c_g)(\partial\varepsilon_i/\partial t)$$

in Eqs. (A.4) as usually valid in the microwave domain [2] and if ω is not too close to the cut-off frequency of the waveguide, we rewrite Eqs. (A.4) in the form

$$\frac{\partial \varepsilon_r}{\partial z} = \frac{2\pi\omega}{c_g} P_i^{10}, \quad \frac{\partial \varepsilon_i}{\partial z} = -\frac{2\pi\omega}{c_g} P_r^{10}. \quad (A.5)$$

With the boundary conditions

$$\varepsilon_r(z=0) = \varepsilon_0, \quad \varepsilon_i(z=0) = 0 \quad (A.6)$$

at the beginning of the absorption cell, we then have the solution for $z = l$, the sample path length

$$\varepsilon_r(t) = \varepsilon_0 + \frac{2\pi\omega l}{c_g}\tilde{P}_i(t),$$
$$\varepsilon_i(t) = -\frac{2\pi\omega l}{c_g}\tilde{P}_r(t), \quad (A.7)$$

where the definition of $\tilde{P}_r(t)$ is analogous to Eq. (4) for $\tilde{P}_i(t)$.

With Eqs. (A.3) and (A.7) the field at the detector ($z = l$) is given by

$$E(\boldsymbol{r}, t) = 2\varepsilon_0 \sin(\pi x/a)\cos(\omega t - k l) + \frac{4\pi\omega l}{c_g}\sin(\pi x/a) \cdot [\tilde{P}_i(t)\cos(\omega t - k l) + \tilde{P}_r(t)\sin(\omega t - k l)]. \quad (A.8)$$

Taking the square of the r.h.s. of Eq. (A.8) and dropping all rapidly varying terms as well as the small terms in $\tilde{P}_i^2$ and $\tilde{P}_r^2$ gives the final result, Eq. (3), for the transient change in output of a square law diode detector due to the absorbing medium.

* Small effects from the change of the wave number k during the course of Stark-switching experiments are not considered here [20].

Acknowledgement

I thank Dipl. Phys. G. Bestmann for designing the control unit for the $\pi, \tau, \pi/2$ pulse sequence experiment, Dr. H. D. Knauth for the PDP-11 computer facilities and the members of the Kiel microwave group for many helpful discussions. The support of the Deutsche Forschungsgemeinschaft and the Fonds der Chemischen Industrie is gratefully acknowledged.

[1] R. H. Schwendeman, Ann. Rev. Phys. Chem. **29**, 537 (1978).
[2] J. C. McGurk, T. G. Schmalz, and W. H. Flygare, Adv. Chem. Phys. **25**, 1 (1974).
[3] H. Mäder, J. Ekkers, W. Hoke, and W. H. Flygare, J. Chem. Phys. **62**, 4380 (1975).
[4] F. Rohart, P. Glorieux, and B. Macke, J. Phys. B: Atom. Molec. Phys. **10**, 3835 (1977).
[5] P. Glorieux, Thesis, Lille 1976.
[6] P. R. Berman, J. M. Levy, and R. G. Brewer, Phys. Rev. A **11**, 1668 (1975).
[7] W. Kauzmann, Kinetic Theory of Gases, W. A. Benjamin, Inc., New York 1966, p. 158–159.
[8] H. Mäder, H. Bomsdorf, and U. Andresen, Z. Naturforsch. **34a**, 850 (1979).
[9] J. C. McGurk, T. G. Schmalz, and W. H. Flygare, J. Chem. Phys. **60**, 4181 (1974).
[10] S. L. Coy, J. Chem. Phys. **63**, 5145 (1975).
[11] W. E. Hoke, D. R. Bauer, J. Ekkers, and W. H. Flygare, J. Chem. Phys. **64**, 5276 (1976).
[12] J. C. McGurk, H. Mäder, R. T. Hofmann, T. G. Schmalz, and W. H. Flygare, J. Chem. Phys. **61**, 3759 (1974).
[13] W. R. MacGillivray, J. Phys. B: Atom Molec. Phys. **9**, 2511 (1976).
[14] G. P. Srivastava, D. Kumar, and A. Kumar, J. Chem. Phys. **66**, 20 (1977).
[15] W. E. Hoke, D. R. Bauer, and W. H. Flygare, J. Chem. Phys. **67**, 3454 (1977).
[16] (a) W. K. Liu and R. A. Marcus, J. Chem. Phys. **63**, 272 (1975); (b) ibid. **63**, 290 (1975); (c) ibid. **63**, 4564 E (1975).

[17] (a) A. F. Turfa, D. E. Fitz, and R. A. Marcus, J. Chem. Phys. **67**, 4463 (1977); (b) A. F. Turka, W. K. Liu, and R. A. Marcus, J. Chem. Phys. **67**, 4468 (1977).
[18] S. Green, J. Chem. Phys. **69**, 4076 (1978).
[19] W. H. Flygare and T. G. Schmalz, Acc. Chem. Res. **9**, 385 (1976).
[20] H. Mäder and H. Bomsdorf, Z. Naturforsch. **33a**, 1493 (1978).
[21] L. Allen and J. H. Eberly, Optical Resonances and Two Level Atoms, J. Wiley and Sons, New York 1975, p. 12ff.
[22] J. D. Jackson, Classical Electrodynamics, J. Wiley and Sons, New York 1975, p. 334ff.
[23] C. Feuillade and J. G. Baker, J. Phys. B: Atom Molec. Phys. **11**, 2501 (1978).